Carbohydrate Polymers 171 (2017) 85–93

Contents lists available at ScienceDirect

Carbohydrate Polymers

journal homepage: www.elsevier.com/locate/carbpol

AOT reverse micelles as versatile reaction media for chitosan nanoparticles synthesis

M. Soledad Orellano[a,b], Carina Porporatto[a], Juana J. Silber[b], R. Darío Falcone[b,*], N. Mariano Correa[b]

[a] Centro de Investigaciones y Transferencia (CONICET), Universidad Nacional de Villa María, Villa María, Córdoba, Argentina
[b] Departamento de Química, Universidad Nacional de Río Cuarto, Agencia Postal # 3, C.P. X5804BYA Río Cuarto, Argentina

ARTICLE INFO

Article history:
Received 9 November 2016
Received in revised form 7 March 2017
Accepted 24 April 2017
Available online 2 May 2017

Keywords:
Chitosan
Nanoparticles
Reverse micelles
AOT
Glutaraldehyde

ABSTRACT

It is known that Chitosan (Ch) can be used in several applications, such as antimicrobial agent or as drug delivery agent. However, being its water dispersibility very low at physiological pH it is necessary to find a way to improve it. One attractive strategy is to synthesize Chitosan Nanoparticles (Ch-NPs). In this work, a versatile method to obtain Ch-NPs with different and controlled sizes, that were successfully prepared by cross-linking reaction of glutaraldehyde and native chitosan inside of *n*-heptane/sodium 1,4-bis-2-ethylhexylsulfosuccinate (AOT)/water reverse micelles (RMs) is presented. Highly monodisperse NPs were synthesized as confirmed by Dynamic Light Scattering (DLS) and Scanning Electron Microscopy (SEM) techniques. The particle size was dependent on the reactants concentration, cross-linking degree and mainly the amount of water inside of the AOT RMs used as nanoreactors. While the cross-linking is quite difficult to control in bulk water, the reaction inside the RMs is more manageable and efficient.

1. Introduction

The elaboration of materials from natural polymers is under intense investigation, as many applications can be addressed such as drug delivery (Swierczewska, Han, Kim, Park, & Lee, 2016), tissue engineering (Suh & Matthew, 2000), diagnostics and imaging (Emerich, Halberstadt, & Thanos, 2007; Nie, Xing, Kim, & Simons, 2007; Solanki, Kim, & Lee, 2008; Tang et al., 2007; Zhao et al., 2004), or for more fundamental aspects of biology (Zou et al., 2016). In this sense, chitosan (Ch) is of particular interest because it is a natural and linear biopolymer obtained from deacetylation of chitin, which is the second more abundant biopolymer after cellulose (Abdul Khalil et al., 2016; Agnihotri, Mallikarjuna, & Aminabhavi, 2004). Moreover, its bioactivity, biodegradability and biocompatibility make this polymer quite appropriate for in vivo applications in medicine (Nagpal, Singh, & Mishra, 2010; Swierczewska et al., 2016; Zou et al., 2016). Structurally, it is a polysaccharide constituted of β-(1,4)-linked glucosamine and *N*-acetyl glucosamine residues (Scheme 1).

Ch has many important properties such as high antimicrobial activity, biocompatibility and low toxicity (Hosseinnejad & Jafari, 2016), which makes it useful for water-quality improvement, cosmetics, drug carriers, pharmaceutics, biomedicine and genetic disease therapy (Nagpal et al., 2010; Swierczewska et al., 2016; Zou et al., 2016). However, despite these desirable characteristics, its application in practical processes is limited because of its poor solubility in water and in most of the conventional organic solvents (Hirase, Higashiyama, Mori, Takahara, & Yamane, 2010; Qian & Zhang, 2010). Ch is a weak base with a pK_a value of about 6.2-7.0, corresponding to the D-glucosamine residues. Therefore, it has low solubility at 7 and higher pH values. In acidic medium, the amino groups are positively charged, resulting in a highly charged polyelectrolyte polysaccharide (Agnihotri et al., 2004; Hirase et al., 2010; Nagpal et al., 2010; Swierczewska et al., 2016; Zou et al., 2016).

One of the methodologies employed to improve the Ch dispersibility in water is to prepare Ch nanoparticles (Ch-NPs) (Chiappisi & Gradzielski, 2015; Elgadir et al., 2015; Swierczewska et al., 2016). Ch-NPs are biocompatible, non-toxic, biodegradable and cationic in nature (Chiappisi & Gradzielski,2015; Elgadir et al., 2015; Swierczewska et al., 2016). Additionally, since nanoparticles (Krasnici et al., 2003; Masarudin, Cutts, Evison, Phillips, & Pigram, 2015; Park et al., 2009) can be easily transported to different body sites and have large surface areas, a growing interest has been directed toward the exploration of the Ch-NPs properties (Mitra, Gaur, Ghosh, & Maitra, 2001). As the size of Ch-NPs plays an

* Corresponding author.
E-mail address: rfalcone@exa.unrc.edu.ar (R.D. Falcone).

http://dx.doi.org/10.1016/j.carbpol.2017.04.074
0144-8617/

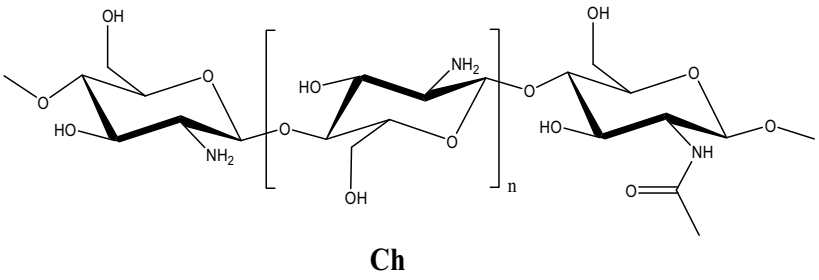

Scheme 1. Schematic representation of Ch.

important role in their application in drug delivery, it is necessary to prepare nanoparticles uniformly sized. In the literature various strategies were reported to produce Ch-NPs with advantages and complications (Abdul Khalil et al., 2016; Kashyap, Xiang, & Heiden, 2015; Nagpal et al., 2010) since their size distribution is very difficult to control. For example, they are usually obtained by physical or covalent cross-linking. Ionic gelation is probably the most used physical cross-linking method, which employ ionic cross-linker such as sodium tripolyphosphate (Kamat, Bodas, & Paknikar, 2016). However, since these particles are formed by electrostatic interactions, changes in the pH of the medium could disrupt its stability (López-León, Carvalho, Seijo, Ortega-Vinuesa, & Bastos-González, 2005; Zhang et al., 2004). Additionally, this method typically yields large sized (100–400 nm) particles with a high degree of polydispersity (Kamat et al., 2016). Consequently, covalent cross-linking seems a more attractive strategy. Thus, in this method cross-linkers (molecules with at least two reactive functional groups) allow the formation of bridges between Ch chains (Jameela & Jayakrishnan, 1995; Pujana, Pérez-álvarez, Iturbe, & Katime, 2012), producing aggregates of Ch interconnected polymers. In order to generate particles in the nanometers range and controlled sizes, an extra procedure is often necessary such as: centrifugation, sonication, filtration or precipitation (Kashyap et al., 2015; Nagpal et al., 2010). Ch is frequently covalent cross-linked using glutaraldehyde (G) which in turn is one of the most effective cross-linking agents (Agnihotri et al., 2004; Baldino, Concilio, Cardea, Marco, & Reverchon, 2015; Berger et al., 2004; Beppu, Vieira, Aimoli, & Santana, 2007; Brunel et al., 2009; Genta, Costantinib, Asti, Conti, & Montanarib, 1998; Jameela & Jayakrishnan, 1995; Mitra et al., 2001; Mi, Kuan, Shyu, Lee, & Chang, 2000; Monteiro & Airoldi, 1999; Nagpal et al., 2010; Poon, Wilson, & Headley, 2014; Park, Kwak, Won, & Yun, 2013; Rivas-Araiza, Alcouffe, Rochas, Montembault, & David, 2010). The cross-linking reaction involves reaction of G with the amino groups of Ch to form an imine cross-link (Scheme 2).

When surfactants molecules are dispersed in a nonpolar solvent, under specific conditions they may self-assemble to form reverse micelles (RMs) aggregates (Correa, Silber, Riter, & Levinger, 2012). Due to the large diversity of nano-environments that these systems provide, such as the micellar core and the interface, RMs have found a wide range of applications in different areas (Correa et al., 2012; Eastoe et al., 2006; Ganguli, Ganguly, & Vaidya, 2010; Parent et al., 2011; Stepankova et al., 2013). These nanoscale aggregates are suitable media for processes that involve hydrophobic and hydrophilic reactants in a variety of chemical and biological reactions (Blach et al., 2014; Correa et al., 2012; Crosio, Correa, Silber, & Falcone, 2016; Durantini, Falcone, Silber, & Correa, 2016; Eastoe et al., 2006) .There are a wide range of surfactants that form RMs, including anionic, cationic, nonionic and zwitterionic molecules (Blach et al., 2014; Correa et al., 2012; Crosio et al., 2016; Durantini et al., 2016; Eastoe et al., 2006; Girardi, Silber, Correa, & Falcone, 2014). Among the anionic surfactants that form RMs in different solvents, the best known is sodium 1,4-bis-2-ethylhexylsulfosuccinate (AOT, Scheme 3) (Correa et al., 2012), which forms spherical RMs in aromatic and aliphatic solvents without the addition of a cosurfactant.

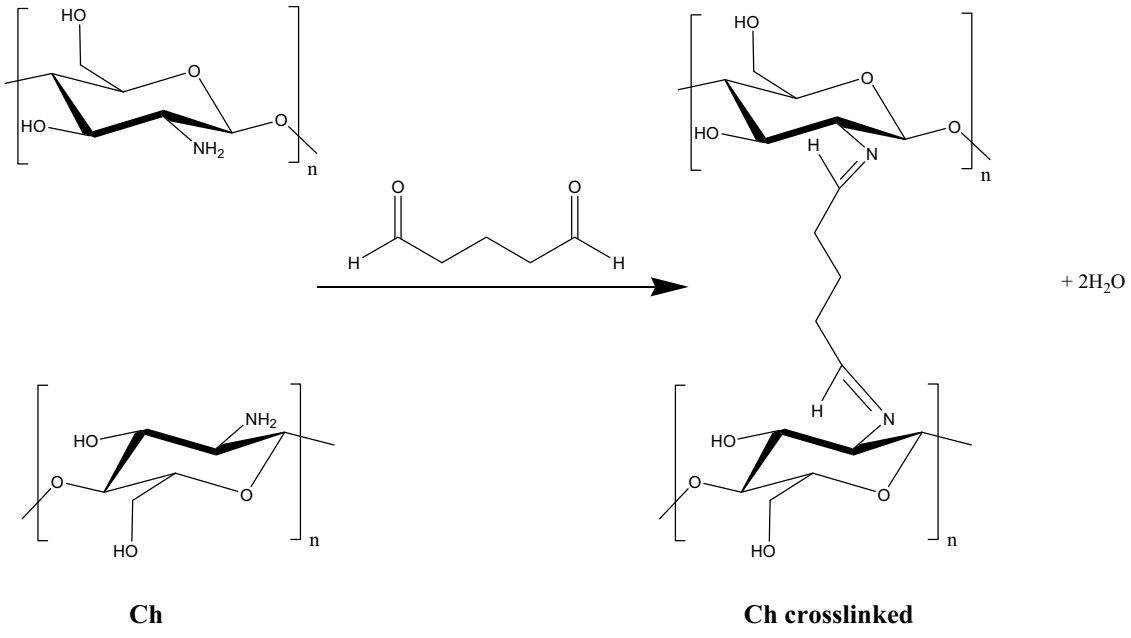

Scheme 2. The cross-linking reaction of native Ch with G.

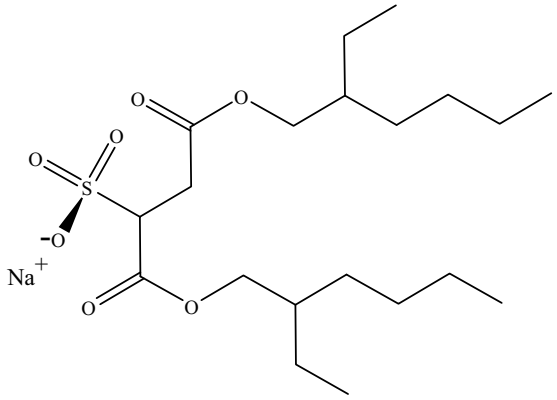

AOT

Scheme 3. Molecular structure of AOT.

Interestingly, variable amount of water can be solubilized depending on different parameters, such as the external solvent and the temperature (De & Maitra, 1995).

One of the most important properties of RMs is their ability to dissolve polar solvents in the inner polar pool and alter substantially its behavior (Blach et al., 2014; Correa et al., 2012; Crosio et al., 2016; Durantini et al., 2016). Particularly, this fact allows the synthesis of different nano-compounds using them as nanoreactors (Gutierrez et al., 2014; Gutierrez, Luna, Correa, Silber, & Falcone, 2015; Lopez-Quintela, 2003; Pileni, 2007). However, few reports have demonstrated the synthesis of covalently cross-linked Ch-NPs (using G as the cross-linker) performed in RMs (Banerjee, Mitra, Kumar Singh, Kumar Sharma, & Maitra, 2002; Brunel, Ve, David, Domard, & Delair, 2008; Kafshgarik, Khorram, Mansouri, Samimi, & Osfouri, 2012; Li et al., 2007; Mitra et al., 2001; Zhi, Wang, & Luo, 2005). Most of them have used non-ionic surfactants such as TX-100 (Li et al., 2007; Liu, Shao, Ge, & Chen, 2007; Mitra et al., 2001; Zhi et al., 2005) and only a few have used AOT as surfactant (Banerjee et al., 2002; Mitra et al., 2001). Maitra et al. (2001) and Banerjee et al. (2002) synthesized Ch-NPs cross-linked with G using as nanotemplate *n*-hexane/AOT RMs at water content (W_0 = [water]/[surfactant]) constant. Quasi-elastic light scattering measurements and transmission electron microscopy (TEM) were used to characterize the NPs. The diameter of the NPs was 30 nm at 10% of cross-linked and 110 nm when all the amine groups are cross-linked (100% cross-linked), working with native Ch of 400 kDa and at W_0 around 20 in both cases. TEM images showed spherical particles but remain aggregated. The authors used just the Ch-NPs for biodistribution in mice and showed that they readily evade the reticoendothelial system and remain in the blood for a considerable amount of time (Banerjee et al., 2002). Additionally, they used the same Ch-NPs as nanocarriers for doxorubicin combined with dextran. The encapsulation of both in Ch-NPs not only reduces the side effects, but also improves its therapeutic efficacy in the treatment of solid tumors (Mitra et al., 2001). However, in both works the effects of water content W_0 on the size distribution of the prepared NPs have not been investigated. Therefore, the aim of the present contribution is to explore if the RMs methodology can be considered as an alternative route to produce reproducible and controlled Ch-NPs. Hence, we study the effect of the water content W_0, cross-linking degree and reactants concentrations on the size, concentration and morphology of Ch-NPs synthesized inside *n*-heptane/AOT/water RMs as nanoreactors.

2. Experimental

2.1. Materials and methods

Sodium 1,4-bis-2-ethylhexylsulfosuccinate (AOT), from Sigma–Aldrich Co. (USA) (>99% purity) was used as received and kept under vacuum to avoid the presence of water. Ultrapure water was obtained from Labonco equipment model 90901-01. *n*-heptane from Sigma–Aldrich Co. (USA) (HPLC quality), was used without prior purification.

Chitosan (Ch) of low molecular weight and glutaraldehyde (G), 50% $^{w}/_{v}$ in water, were purchased from Sigma–Aldrich Co. (USA). The deacetylation degree of Ch measured by FT-IR (Baxter, Dillion, Taylor, & Roberts, 1992; Chen, Hsu, Huang, Tsai, & Chen, 2011) was 79% which is in good agreement with the value reported by the supplier (75–85%). Static light scattering was used to measure the weight-average molecular weight (M_w) of the Ch (Guo, Lin, & Yu, 2002; Nakata, 1997; Pa & Yu, 2001; Sorlier, Rochas, Morfin, Viton, & Domard, 2003). Several solutions of Ch in acetic acid (1% $^{v}/_{v}$) in a range of concentrations i.e 1.7–7.3 mg/ml, were prepared and filtrated through a 0.45 μm nylon filter (Millipore, USA), prior to the light scattering measuring. The scattered light intensity of the solutions was measured by a Malvern light scattering photometer (Malvern 4700 with goniometer) at 488 nm. The Mw (equal to 212.7 kDa) was calculated from the Zimm plot processed by Malvern software (version 1.61 for Windows). Refractive index increments (*dn/dc*) of Ch solutions equaled 0.105 ml/mg and were determined by a differential refractometer (Brookhaven Instruments Corporation, BI-DNDCW model) with a tungsten lamp operating at 470 nm and T = 30 °C.

2.2. Preparation of AOT RMs solutions

Stock solutions of AOT (0.1 M) in *n*-heptane were prepared by mass and volumetric dilution. Aliquots of these stock solutions were used to make individual RMs solutions with different amount of water, defined as W_0 = [water]/[AOT]. The incorporation of water and reactants into each micellar solutions were performed using calibrated microsyringes. Thus, for example, to prepare 10 ml of AOT RMs solution at W_0 = 20 and [AOT] = 0.1 M, 0.36 ml of water was added. All the resulting solutions were clear with a single phase and they were used in the synthesis experiments.

2.3. Preparation of cross-linked Ch-NPs in AOT RMs

To 10 ml of 0.1 M AOT/*n*-heptane solution, 0.25 ml of 0.1% $^{w}/_{v}$ native Ch solution in hydrochloric acid (1×10^{-2} M), 2.5 μl of 0.01% $^{w}/_{v}$ G aqueous solution and the extra amount of water (considering additive aqueous solutions) to achieve the desired W_0 were added, with continuous stirring at room temperature. The final solution was homogenous, optically transparent and stable over time. The system was left, under stirring, overnight at room temperature. The above method is to produce Ch-NPs with 10% cross-linkage (Banerjee et al., 2002). It is important to note that in absence of AOT, Ch and G are not soluble in *n*-heptane. In order to separate the nanoparticles from the RMs media, the following steps were performed: *n*-heptane was evaporated in a rotary evaporator and the dry mass (Ch-NPs and AOT surfactant) was dissolved in pure water. The aqueous solution containing Ch-NPs was purified by dialysis for 7 days against pure water using a dialysis bag (14 kDa cut off, Sigma-Aldrich Co, USA). The dialyzed solution was lyophilized (Labconco FreeZone 6 Liter Freeze Dry System with Stoppering Tray Dryer) to dry powder for subsequent use. The mass of dry Ch-NPs obtained after the process was around 40% of the chitosan used in the reaction mixture. Lyophilized Ch-NPs were easily dispersible in pure

water. To produce Ch-NPs with a different cross-linking degree, different amount of G were added to the RMs solution.

2.4. DLS experiments

The apparent diameters of Ch-NPs were determined by dynamic light scattering (DLS, Malvern 4700 with goniometer). The laser used is an argon-ion operating at 488 nm and the methodology employed was described elsewhere (Crosio et al., 2016; Girardi et al., 2014). The samples were filtered prior to the experiments using an Acrodisc with 0.45 μm nylon membrane (Sigma). To obtain statistic reliable results, 30 independent size measurements were taken for each of the samples. The scattering angle used was ninety degrees. CONTIN was used as the algorithm to obtain the apparent hydrodynamic diameter values. The polydispersity found for the different solutions investigated is always less than 5%.

2.5. SEM experiments

Scanning electron microscopy (SEM) images of Ch-NPs were obtained with a SIGMA (Carl Zeiss) field emission scanning electron microscope (FE-SEM), using secondary electron irradiation and 8 kV with 100 × magnification. SEM experiments were carried out in the Laboratorio de Microscopía Electrónica y Análisis por Rayos X (LAMARX), from the Facultad de Matemática, Astronomía y Física (FAMAF), Universidad Nacional de Córdoba, Argentina.

2.6. FT-IR analysis

Fourier transform infrared (FT-IR) spectra were recorded with a Nicolet IMPACT400 FT-IR spectrometer. Native Ch and Ch-NPs samples were recorded in the range 400–4000 cm^{-1} using KBr pellets at room temperature. Each sample was obtained by co-adding 200 spectra at a resolution of 0.5 cm^{-1}.

3. Results and discussion

To search for the factors that impact on the Ch-NPs formation upon confinement on RMs, we evaluate the effect of the AOT RMs, the water content (W_0) and reactant concentrations on the synthesized particles using Dynamic Light Scattering (DLS) and Scanning Electron Microscopy (SEM) techniques.

3.1. Synthesis and characterization of Ch-NPs in AOT RMs

Ch-NPs were successfully formed inside AOT RMs through covalent cross-linking reaction (Scheme 2) of native Ch with G acting as a cross-linker as the FT-IR experiments show. Thus, the cross-linking reaction involves the aldehyde function (–CHO) of G with the amino groups (–NH_2) of Ch to form a stable imine bonds as it was reported before (Guyomard-Lack, Buchtova, Humbert, & Bideau, 2015; Monsan, Puzo, & Mazarguil, 1975; Monsan, 1978; Monteiro & Airoldi, 1999). FT-IR studies of Ch and Ch-NPs were performed to characterize the chemical structure of nanoparticles and the results are shown in Fig. 1. It is important to denote that Ch-NPs were synthesized in *n*-heptane/AOT/water RMs at [AOT] = 0.1 M and W_0 = 10 and the FT-IR data correspond to the NPs lyophilized after removal of AOT (see experimental procedure).

As it can be seen, in Ch the strong peaks in the range 3400–3200 cm^{-1} (Fig. 1A) correspond to combined peaks of hydroxyl and intramolecular hydrogen bonding. Primary amines also show sharp absorption at 3500 and 3400 cm^{-1} arising from the asymmetric and symmetric stretching of the N—H bonds, but the peak appears broad here due to the superimposed peaks of O—H stretching (Qi, Xu, Jiang, Hu, & Zou, 2004). Thus, Ch shows O—H and N—H stretching frequencies at 3396 cm^{-1}. Fig. 1B shows

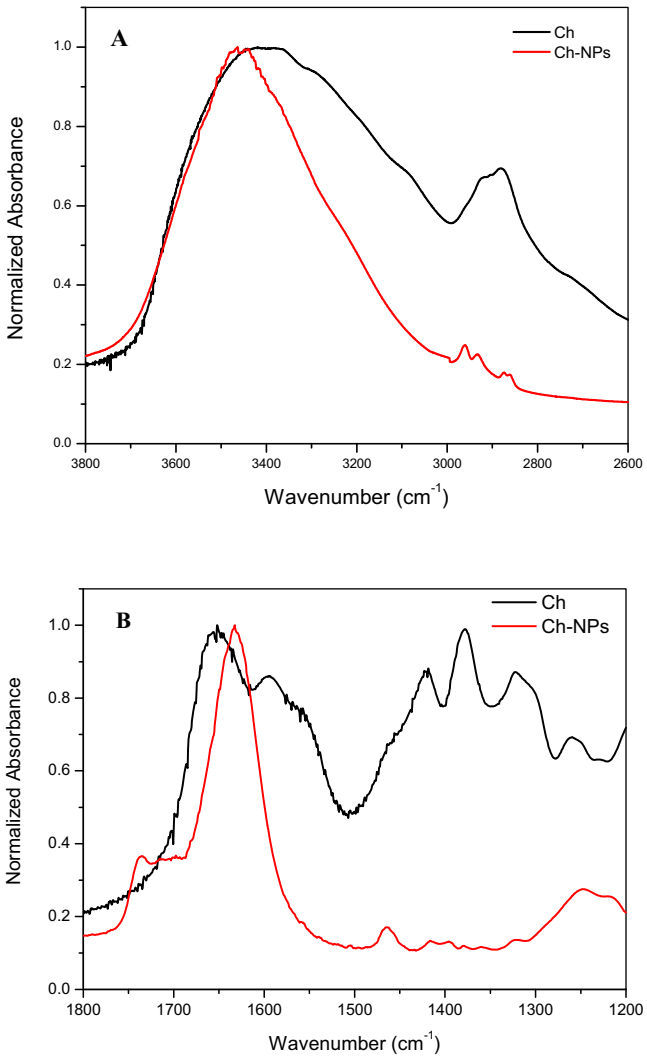

Fig. 1. Normalized FT-IR spectra of Ch and Ch-NPs cross-linked with G in the region of 3800–2600 cm^{-1} (A) and 1800–1200 cm^{-1} (B). Ch = 0.1% $^{w}/_{v}$, G = 0.01% $^{w}/_{v}$. Ch:G = 10:1.

the asymmetric C—O vibrational band at 1651 cm^{-1} which is assigned to the presence of the carbonyl in the amide group in Ch (Qi et al., 2004; Zhou, Jiang, Lee, & Yue, 2013). The IR band at 1594 cm^{-1} corresponds mainly to deformations of the primary amine groups (δ NH_2) (Poon et al., 2014; Qi et al., 2004). The adsorption peaks at 1378 cm^{-1} (—C—O— stretching of primary alcoholic group), 1151 cm^{-1} (asymmetric stretching of —C—O—C— bridge), 1076 cm^{-1} (primary O—H group attached to —CH_2OH) (Kajjari, Manjeshwar, & Aminabhavi, 2013) and 1031 cm^{-1} (C—N bond), also can be identified (Zhou et al., 2013) (Fig. 1B).

For cross-linked Ch-NPs, a new peak at 1634 cm^{-1} can be observed in Fig. 1B, which corresponds to stretching vibrations of imine bond (C=N) (Liu et al., 2007; Poon et al., 2014; Zhou et al., 2013). This strong peak indicates the formation of Schiff's base as a result of the reaction between carbonyl group of G and amine group of Ch chains (Banerjee et al., 2002; Liu et al., 2007; Poon et al., 2014; Zhou et al., 2013) Additionally, the reduction of the δ (NH_2) band at 1594 cm^{-1} is attributed to the cross-linking with G (Monteiro & Airoldi, 1999; Qi et al., 2004).

The apparent hydrodynamic diameter (D_{app}) values of the Ch-NPs samples in pure water were obtained by DLS technique, under different conditions as it will be explained later. The Ch-NPs dispersed in water was monitored as a function of time for

Table 1
Comparison of the sizes (D_{app}) and polydispersity index (PDI) values of the cross-linking reaction performed in AOT RMs and bulk water. Ch = 0.1% $^{w}/_{v}$, G = 0.01% $^{w}/_{v}$. Ch:G = 10:1. [AOT] = 0.1 M. W_0 = 10. T = 25 °C.

Media used as nanoreactor	D_{app}[a] (nm)	PDI
bulk water	62 ± 2 (3.8%) 557 ± 17 (68.6%) 7630 ± 229 (14.8%) 138822 ± 4165 (12.8%)	1
n-heptane/AOT/water RMs	90 ± 3 (100%)[b]	0.2

[a] Values in parentheses show the% population obtained from the DLS analysis.
[b] Data corresponding to the NPs dissolved in water after removal of RMs.

Table 2
D_{app} and PDI values obtained in *n*-heptane/AOT/water RMs after Ch-NPs formation and in absence of reactants. [AOT] = 0.1 M. W_0 = 10. T = 25 °C.

System	D_{app} (nm)	PDI
AOT RMs containing Ch-NPs after overnight reaction[a]	8.4 ± 0.5	0.07
AOT RMs without reactants	7.5 ± 0.5[b]	0.05

[a] Ch = 0.1% $w/_v$, G = 0.01% $^{w}/_{v}$. Ch:G = 10:1.
[b] Data collected from Gutierrez et al., 2014.

all samples in several succeeding days and practically no changes were observed in the samples particle sizes with time (results not shown).

In order to evaluate the effect of the RMs on the Ch-NPs formation, the cross-linking reaction was compared when it is run in AOT RMs and in water. In this sense, Table 1 summarizes the D_{app} values of the Ch-NPs in water but synthesized directly in bulk water (absence of RMs) or in *n*-heptane/AOT/water RMs at W_0 = 10. It is important to note that the data corresponding to RMs represent the NPs suspended in water after removal of the organized media (See detailed procedure in experimental section). In both cases the ratio Ch:G was kept constant to maintain the same cross-linking reaction degree.

As it can be seen, the D_{app} values are very different depending on the media used for the reaction. Thus, is possible to detect small nanoparticles with diameter around 90 nm when AOT RMs are used as nanoreactor. On the other hand, in bulk water the reaction produce a cross-linking polymer with very heterogeneous sizes (60–130000 nm) denoting that the cross-liking reaction is completely random in absence of organized system. Additionally, the PDI values were used as an indicator for the NPs stability and for the uniformity of the distribution sizes. It is known that, a low PDI value indicates more monodisperse particles, while higher PDI values show lower particle stability, the presence of aggregates or even the absence of particles. Thus, when the Ch-NPs are prepared in RMs and then re-dispersed in water, the samples consisting of evenly sized particles have low PDI values where only one population is detected. When the cross-linking reaction is performed directly in bulk water, the samples have a non-statistical PDI value of 1 with a wider range of sizes which probably reflect the absence of nanoparticles. Consequently, the presences of RMs help to organize the NPs formation in a well-ordered way, producing Ch-NPs with a small and uniform size. In this sense, the confinement of Ch inside AOT RMs could orientate the NH_2 groups of Ch near to the anionic interface which favors the cross-linking reaction.

Table 1 denotes another interesting fact: the D_{app} value of the Ch-NPs prepared into RMs at W_0 = 10 does not represent the "real" AOT RMs droplets size at this water content. In Table 2 are showed the D_{app} values obtained using RMs as template in the cross-linking reaction and in the RMs in absence of reactants. As it is well known, the diameter of *n*-heptane/AOT/water RMs are a few nanometers (Gutierrez et al., 2014) while the Ch-NPs show size values around 90 nm (Table 1).

Table 3
Size and polydispersity index values of Ch-NPs synthesized in *n*-heptane/AOT/water RMs at different W_0. Ch = 0.1% $^{w}/_{v}$, G = 0.01% $^{w}/_{v}$. Ch:G = 10:1. [AOT] = 0.1 M. T = 25 °C.

W_0	D_{app} (nm)[a]	PDI
5	75 ± 3	0.3
10	90 ± 3	0.2
20	109 ± 4	0.2
25	137 ± 5	0.2

[a] Data corresponding to the NPs dissolved in water after removal of RMs.

Table 4
Size and polydispersity index values of Ch-NPs synthesized in *n*-heptane/AOT/water RMs at different G concentrations and W_0 = 20. Ch = 0.1% $^{w}/_{v}$, [AOT] = 0.1 M. T = 25 °C.

G (% $^{w}/_{v}$)	Ch:G	D_{app} (nm)[a]	PDI
0.01	10:1	109 ± 4	0.2
0.05	2:1	66 ± 2	0.2

[a] Data corresponding to the NPs dissolved in water after removal of RMs.

Table 5
Size and polydispersity index of Ch-NPs synthesized in AOT RMs at different reactants concentrations and W_0. Ch:G = 10:1. [AOT] = 0.1 M. T = 25 °C.

Ch (% $^{w}/_{v}$)	G (% $^{w}/_{v}$)	W_0	D_{app} (nm)[a]	PDI
0.10	0.010	5	75 ± 3	0.3
1.25	0.125	5	134 ± 4	0.2
0.10	0.010	20	109 ± 4	0.2
0.25	0.025	20	181 ± 6	0.2

[a] Data corresponding to the NPs dissolved in water after removal of RMs.

As it can be seen from Tables 1 and 2, the Ch-NPs are around twelve times larger than the corresponding template (90 nm vs 7.5 nm). Moreover, the presence of Ch-NPs inside RMs does not disturb the organized media, showing similar sizes (8.4 vs 7.5 nm) independently if the RMs have NPs or only water entrapped.

The fact that Ch-NPs show different sizes after removal from the RMs template (Table 1) or inside RMs (Table 2), even that both are finally dissolved in bulk water, can be explained considering two backgrounds: i) Ch-NPs, due to strong hydrogen bond interactions, have the ability to incorporate water inside the particle forming hydrogel solutions (Baldino et al., 2015; Berger et al., 2004; Bodnar, Hartmann, & Borbely, 2005; Rivas-Araiza et al., 2010) and is not surprising to observe large NPs in water (swollen state) (Bodnar et al., 2005; Bodnar, Hartmann, & Borbely, 2006; De Moura, Aouada, & Mattoso, 2008; Kajjari et al., 2013; Pujana et al., 2012; Zhou et al., 2013). ii) it is known that the water properties inside the RMs are completely different that those in bulk solution, due to confinement but mainly by interaction with the interface (Correa & Levinger, 2006; Cringus et al., 2007; Piletic, Tan, & Fayer, 2005). For example, due to hydrogen bond interaction between the entrapped water and the SO_3^- group of AOT at the interface, the water molecules inside AOT RMs show enhanced electron donor ability but reduced hydrogen bond donor ability compared with bulk water (Correa et al., 2012). These facts have tremendous impact when RMs are used as nanoreactors (Gutierrez et al., 2014). Thus, as Tables 1 and 2 show, the smaller sizes of Ch-NPs obtained in AOT RMs (not in swollen state) than in bulk water can be due to the inefficacy to interact with the entrapped water. However, the electrons pairs of the oxygen in the water entrapped can provide extra stabilization when the NH_2 groups of native Ch are near to anionic interface. After the RMs removal, Ch-NPs recover the swollen state.

3.2. *Effect of water content (W_0) on the size of Ch-NPs*

In order to explore the effect that the water pool size has on the Ch-NPs structure, we performed the synthesis at different water

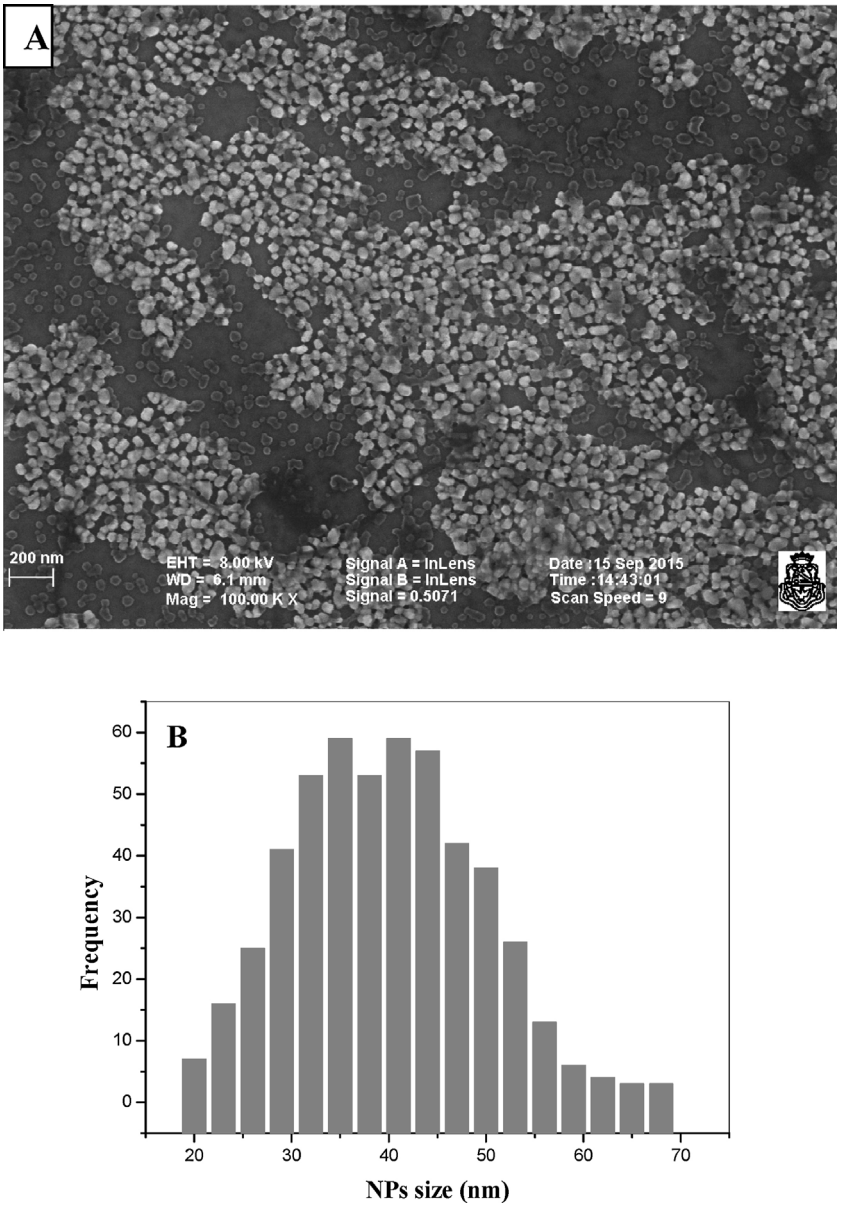

Fig. 2. A) SEM image and B) sizes distribution of Ch-NPs synthesized in *n*-heptane/AOT/water RMs at $W_0 = 5$, Ch: 1.25% $^{w}/_{v}$, G: 0.125% $^{w}/_{v}$. [AOT] = 0.1 M. Ch:G = 10:1. Scale bar = 200 nm and magnification = 100 ×.

contents. The D_{app} values obtained are reported in Table 3 and plotted in Fig. S1 (Supplementary information section).

The data show that there is a clear tendency to increase the Ch-NPs sizes when the W_0 increases. If we consider that the cross-linking reaction occurs in the water pool, is expectable that if the nanoreactor size increases the final particle size also increases. However, as it was mentioned before the final size of the Ch-NPs suspended in water is clearly different to the nanoreactor size. Apparently, the cross-linking degree is not the same at all the W_0 evaluated. When the droplet sizes decreases and the cross-linking degree increases, the NPs are less hydrophilic and more compact (less free volume inside) (Bodnar et al., 2005). We think that when the entrapped water content is low, more cross-linked and smaller are the Ch-NPs due to a better location of the reactants. When the W_0 is higher the probable interaction between the NH_2 groups and the anionic interface is diminished by the water added, producing a native Ch less well-ordered, decreasing the cross-linking reaction efficiency and generating larger particles.

The quasi-linear relationship between the Ch-NPs sizes and W_0 (Fig. S1) is very interesting in order to think about future applications of these NPs. Thus, different sizes (and different applications) can be obtained just changing the amount of entrapped water. It is important to note that the ability to produce different size and monodisperse particles becomes in the RMs method as an advantage in comparison with other more simple (Abdul Khalil et al., 2016; Kashyap et al., 2015; Nagpal et al., 2010) but not so versatile methods like the presented in this work.

3.3. *Effect of the cross-linker concentration on the size of Ch-NPs*

The synthesis of Ch-NPs inside AOT RMs was also studied varying the amount of G used to prepare the particles. In Table 4 the data obtained from DLS changing the G concentration but keeping constant the amount of Ch, are presented.

As it can be observed when the amount of G increase (ratio Ch:G decrease) although the PDI values are similar in both cases, the

size of the NPs decrease from 109 nm to 66 nm. The same behavior was observed before for Ch-NPs but using others cross-linker and methodologies to prepare the particles (Bodnar et al., 2005; Bodnar et al., 2006; De Moura et al., 2008; Tallury et al., 2009). A possible explanation is that more cross-linked NPs are smaller (Bodnar et al., 2006) because less free volume between the Ch chains is available and a reduction of the free primary amino groups on the polymer which produce less hydrophilic NPs. This also means that increasing the cross-linking reaction more Ch chains are connected and there is less space for the water molecules to interact with the polar groups, thus decreases the ability of the particles to be hydrated. On the contrary, Ch-NPs less cross-linked are more hydrophilic and consequently larger.

3.4. Effect of the Ch concentration on the size of Ch-NPs

In order to extend the Ch-NPs characterization, the amount of native Ch in the cross-linking reaction was evaluated (Table 5). As it can be observed from Table 5 the reactants concentration was varied but the Ch:G ratio was maintained constant. Additionally, this experiment was performed a two different W_0 (5 and 20). From Table 5, several facts can be analyzed: i) increasing the reactants concentration increase the Ch-NPs sizes at W_0 constant; ii) the water content of the RMs has more influence in the final NPs than the amount of reactants used.

Interestingly, the result at $W_0 = 20$ shows that the NPs size increases from 109 nm to 181 nm (1.7 times) when the Ch concentration changes from 0.1 to 0.25% $^{w}/_{v}$ (2.5 times). However, if the water content is smaller ($W_0 = 5$), similar NPs size increment (1.8 times) is obtained, even if the Ch concentration is 12.5 times larger (0.1–1.25% $^{w}/_{v}$). Apparently, the presence of more reactants to interact in a smaller region prevents the cross-linking reaction. Thus, in order to obtain a specific NPs size both the amount of reactants and the water content are factors to consider in the formation.

With regard to the morphology of the Ch-NPs synthesized, SEM experiments were performed. Fig. 2A and B shows the SEM image and the size distribution of Ch-NPs dissolved in pure water but synthesized in *n*-heptane/AOT/water RMs ($W_0 = 5$) as template.

As it is observed in Fig. 2A, a quasi-spherical morphology is found and although the synthesis is performed at high reactant concentration but small W_0, no aggregation of Ch-NPs is detected.

It is remarkable from Fig. 2B that the sizes of Ch-NPs obtained from SEM was smaller (40 ± 9 nm) than those obtained from DLS analysis showed in Table 3 for the same W_0 (75 ± 3 nm). In this regard, it must be taking into account that DLS measures the hydrodynamic diameter of particles in solution (swollen state) (Bodnar et al., 2005; Bodnar et al., 2006; De Moura et al., 2008), whereas SEM sizes arise from direct inspection in absence of solvent (Goldstein et al., 1992). Thus, the differences in sizes can be due to the hydration level of the particles.

4. Conclusions

Ch-NPs were successfully prepared by cross-linking reaction of G and native Ch inside of AOT RMs as an alternative methodology to produce highly monodisperse NPs. NPs synthesized were confirmed by both DLS and SEM analysis, where the Ch-NPs present a very homogeneous morphology with predominantly spherical and quite uniform particles size distribution. The particle size is dependent on the reactants concentration, cross-linking degree and mainly the amount of water of the AOT RMs used in the nanoparticle preparation. This behavior is due to efficiency of the cross-linking reaction inside RMs which is not possible to control in homogeneous media. In this sense, the possibility to generate Ch-NPs with different sizes is of key importance to optimize their uses in several applications such as antimicrobial agent (Hosseinnejad & Jafari, 2016), delivery system of drugs (Nagpal et al., 2010) or antigens (Gregory, Titball, & Williamson, 2013) in medicine or in agriculture (Kashyap et al., 2015). Thus, different sizes (for different applications) can be obtained, for example, just changing the amount of water entrapped. Interestingly, the ability to produce different size and monodisperse particles shows that the RMs method has several advantages in comparison with other may be simpler, but not so versatile methods like the presented in this work.

Acknowledgements

Financial support from Consejo Nacional de Investigaciones Científicas y Técnicas (CONICET, PIP CONICET 112-201101-00204), Universidad Nacional de Río Cuarto, Agencia Nacional de Promoción Científica y Técnica (PICT 2012-0232, PICT 2012-0526 and PICT 2015-0585), and Ministerio de Industria, Comercio, Minería y Desarrollo Científico Tecnológico de Córdoba (PID-2013) are gratefully acknowledged. C.P., N.M.C., J.J.S. and R.D.F. hold a research position at CONICET. M.S.O. thanks CONICET for a research fellowship. The authors thank Dr. Alejo C. Carreras for his help in the SEM experiments.

Appendix A. Supplementary data

Supplementary data associated with this article can be found, in the online version, at http://dx.doi.org/10.1016/j.carbpol.2017.04.074.

References

Abdul Khalil, H. P. S., Saurabh, C. K., Adnan, A. S., Nurul Fazita, M. R., Syakir, M. I., Davoudpour, Y., & Dungani, R. (2016). A review on chitosan-cellulose blends and nanocellulose reinforced chitosan biocomposites: Properties and their applications. *Carbohydrate Polymers*, *150*, 216–226. http://doi.org/10.1016/j.carbpol.2016.05.028

Agnihotri, S. A., Mallikarjuna, N. N., & Aminabhavi, T. M. (2004). Recent advances on chitosan-based micro- and nanoparticles in drug delivery. *Journal of Controlled Release*, *100*(1), 5–28. http://doi.org/10.1016/j.jconrel.2004.08.010

Baldino, L., Concilio, S., Cardea, S., Marco, I., & Reverchon, E. (2015). The Journal of Supercritical Fluids Complete glutaraldehyde elimination during chitosan hydrogel drying by SC-CO 2 processing. *The Journal of Supercritical Fluids*, *103*, 70–76. http://doi.org/10.1016/j.supflu.2015.04.020

Banerjee, T., Mitra, S., Kumar Singh, A., Kumar Sharma, R., & Maitra, A. (2002). Preparation, characterization and biodistribution of ultrafine chitosan nanoparticles. *International Journal of Pharmaceutics*, *243*(1–2), 93–105. http://doi.org/10.1016/S0378-5173(02)00267-3

Baxter, A., Dillion, M., Taylor, K., & Roberts, G. (1992). Improved method for I. R. determination of the degree of acetylation of chitosan. *International Journal of Biological Macromolecules*, *14*, 166–169.

Beppu, M. M., Vieira, R. S., Aimoli, C. G., & Santana, C. C. (2007). Crosslinking of chitosan membranes using glutaraldehyde: Effect on ion permeability and water absorption. *Journal of Membrane Science*, *301*, 126–130. http://doi.org/10.1016/j.memsci.2007.06.015

Berger, J., Reist, M., Mayer, J. M., Felt, O., Peppas, N. A., & Gurny, R. (2004). Structure and interactions in covalently and ionically crosslinked chitosan hydrogels for biomedical applications. *European Journal of Pharmaceutics and Biopharmaceutics*, *57*, 19–34. http://doi.org/10.1016/S0939-6411(03)00161-9

Blach, D., Pessêgo, M., Silber, J. J., Correa, N. M., García-Río, L., & Falcone, R. D. (2014). Ionic liquids entrapped in reverse micelles as nanoreactors for bimolecular nucleophilic substitution reaction. Effect of the confinement on the chloride ion availability. *Langmuir: The ACS Journal of Surfaces and Colloids*, *30*(41), 12130–12137. http://doi.org/10.1021/la501496a

Bodnar, M., Hartmann, J. F., & Borbely, J. (2005). Preparation and characterization of chitosan-based nanoparticles. *Biomacromolecules*, *6*(5), 2521–2527. http://doi.org/10.1021/bm0502258

Bodnar, M., Hartmann, J. F., & Borbely, J. (2006). Synthesis and study of cross-linked chitosan-N-poly (ethylene glycol). *Nanoparticles*, 3030–3036.

Brunel, F., Véron, L., David, L., Domard, A., & Delair, T. (2008). A novel synthesis of chitosan nanoparticles in reverse emulsion. *Langmuir*, *24*(20), 11370–11377. http://doi.org/10.1021/la801917a

Brunel, F., Véron, L., Ladavière, C., David, L., Domard, A., & Delair, T. (2009). Synthesis and structural characterization of chitosan nanogels. *Langmuir: The ACS Journal of Surfaces and Colloids*, *25*(16), 8935–8943. http://doi.org/10.1021/la9002753

Chen, W. Y., Hsu, C. H., Huang, J. R., Tsai, M. L., & Chen, R. H. (2011). Effect of the ionic strength of the media on the aggregation behaviors of high molecule weight chitosan. *Journal of Polymer Research*, *18*(6), 1385–1395. http://doi.org/10.1007/s10965-010-9543-9

Chiappisi, L., & Gradzielski, M. (2015). Co-assembly in chitosan-surfactant mixtures: Thermodynamics, structures, interfacial properties and applications. *Advances in Colloid and Interface Science*, *220*, 92–107. http://doi.org/10.1016/j.cis.2015.03.003

Correa, N. M., & Levinger, N. E. (2006). What can you learn fom a molecular probe? New insights on the behavior of C343 in homogeneous solutions and AOT reverse micelles. *Journal of Physical Chemistry B*, *110*(26), 13050–13061. http://doi.org/10.1021/jp0572636

Correa, N. M., Silber, J. J., Riter, R. E., & Levinger, N. E. (2012). Nonaqueous polar solvents in revers micelle systems. *Chemical Reviews*, *112*, 4569–4602. http://doi.org/10.1021/cr200254q

Cringus, D., Bakulin, A., Lindner, J., Vöhringer, P., Pshenichnikov, M. S., & Wiersma, D. A. (2007). Ultrafast energy transfer in water-AOT reverse micelles. *The Journal of Physical Chemistry B*, *111*(51), 14193–14207. http://doi.org/10.1021/jp0723158

Crosio, M. A., Correa, N. M., Silber, J. J., & Falcone, R. D. (2016). A protic ionic liquid, when entrapped in cationic reverse micelles, can be used as a suitable solvent for a bimolecular nucleophilic substitution reaction. *Organic & Biomolecular Chemistry*, 3170–3177. http://doi.org/10.1039/c5ob02664d

De, T. K., & Maitra, A. (1995). Solution behaviour of Aerosol OT in non-polar solvents. *Advances in Colloid and Interface Science*, *59(C*, 95–193. http://doi.org/10.1016/0001-8686(95)80005-N

de Moura, M. R., Aouada, F. A., & Mattoso, L. H. C. (2008). Preparation of chitosan nanoparticles using methacrylic acid. *Journal of Colloid and Interface Science*, *321*(2), 477–483. http://doi.org/10.1016/j.jcis.2008.02.006

Durantini, A. M., Falcone, R. D., Silber, J. J., & Correa, N. M. (2016). Effect of confinement on the properties of sequestered mixed polar solvents: Enzymatic catalysis in nonaqueous 1,4-bis-2-ethylhexylsulfosuccinate reverse micelles. *ChemPhysChem*, *17*(11), 1678–1685. http://doi.org/10.1002/cphc.201501190

Eastoe, J., Gold, S., Rogers, S., Wyatt, P., Steytler, D. C., Gurgel, A., & Enick, R. M. (2006). Designed CO2-philes stabilize water-in-carbon dioxide microemulsions. *Angewandte Chemie—International Edition*, *45*(22), 3675–3677. http://doi.org/10.1002/anie.200600397

Elgadir, M. A., Uddin, M. S., Ferdosh, S., Adam, A., Chowdhury, A. J. K., & Sarker, M. Z. I. (2015). Impact of chitosan composites and chitosan nanoparticle composites on various drug delivery systems: A review. *Journal of Food and Drug Analysis*, *23*(4), 619–629. http://doi.org/10.1016/j.jfda.2014.10.008

Emerich, D. F., Halberstadt, C., & Thanos, C. (2007). Role of nanobiotechnology in cell-based nanomedicine: A concise review. *Journal of Biomedical Nanotechnology*, *3*(3), 235–244.

Ganguli, A. K., Ganguly, A., & Vaidya, S. (2010). Microemulsion-based synthesis of nanocrystalline materials. *Chemical Society Reviews*, *39*(2), 474–485.

Genta, I., Costantini, M., Asti, A., Conti, B., & Montanari, L. (1998). Influence of glutaraldehyde on drug release and mucoadhesive properties of chitosan microspheres. *Carbohydrate Polymers*, *36*(2), 81–88. http://doi.org/10.1016/S0144-8617(98)00022-8

Girardi, V. R., Silber, J. J., Correa, N. M., & Falcone, R. D. (2014). The use of two non-toxic lipophilic oils to generate environmentally friendly anionic reverse micelles without cosurfactant. Comparison with the behavior found for traditional organic non-polar solvents. *Colloids and Surfaces A: Physicochemical and Engineering Aspects*, *457*(1), 354–362. http://doi.org/10.1016/j.colsurfa.2014.05.077

Goldstein, J. I., Newbury, D. E., Echlin, P., Joy, D. C., Fiori, C., & Lifshin, E. (1992). *Scanning electron microscopy and X-ray microanalysis*. New York: Plenum.

Gregory, A. E., Titball, R., & Williamson, D. (2013). Vaccine delivery using nanoparticles. *Frontiers in Cellular and Infection Microbiology*, *3*(March), 13. http://doi.org/10.3389/fcimb.2013.00013

Guo, H., Lin, H., & Leon Yu, T. (2002). Dilute solution properties of chitosan in propionic acid aqueous solutions. *Journal of Macromolecular Science, Part A*, *39*(8), 837–852. http://doi.org/10.1081/MA-120005804

Gutierrez, J. A., Falcone, R. D., Lopez-Quintela, M. A., Buceta, D., Silber, J. J., & Correa, N. M. (2014). On the investigation of the droplet–droplet interactions of sodium 1,4-bis(2-ethylhexyl) sulfosuccinate reverse micelles upon changing the external solvent composition and their impact on gold nanoparticle synthesis. *European Journal of Inorganic Chemistry*, *12*, 2095–2102. http://doi.org/10.1002/ejic.201301612

Gutierrez, J. A., Luna, M. A., Correa, N. M., Silber, J. J., & Falcone, R. D. (2015). The impact of the polar core size and external organic media composition on micelle–micelle interactions: The effect on gold nanoparticle synthesis. *New J. Chem.*, *39*(11), 8887–8895. http://doi.org/10.1039/C5NJ01126D

Guyomard-Lack, A., Buchtová, N., Humbert, B., & Le Bideau, J. (2015). Ion segregation in an ionic liquid confined within chitosan based chemical ionogels. *Phys. Chem. Chem. Phys.*, *17*(37), 23947–23951. http://doi.org/10.1039/C5CP04198H

Hirase, R., Higashiyama, Y., Mori, M., Takahara, Y., & Yamane, C. (2010). Hydrated salts as both solvent and plasticizer for chitosan? *Carbohydrate Polymers*, *80*(3), 993–996.

Hosseinnejad, M., & Jafari, S. M. (2016). Running Title: Antimicrobial properties of chitosan. *International Journal of Biological Macromolecules*.

Jameela, S. R., & Jayakrishnan, A. (1995). Glutaraldehyde cross-linked chitosan microspheres as a long acting biodegradable drug delivery vehicle: Studies on the in vitro release of mitoxantrone and in vivo degradation of microspheres in rat muscle. *Biomaterials*, *16*(10), 769–775. http://doi.org/10.1016/0142-9612(95)99639-4

Kafshgarik, M. H., Khorram, M., Mansouri, M., Samimi, A., & Osfouri, S. (2012). Preparation of alginate and chitosan nanoparticles using a new reverse micellar system. *Iranian Polymer Journal*, *21*(2), 99–107.

Kajjari, P. B., Manjeshwar, L. S., & Aminabhavi, T. M. (2013). Novel blend microspheres of poly(vinyl alcohol) and succinyl chitosan for controlled release of nifedipine. *Polymer Bulletin*, *70*(12), 3387–3406. http://doi.org/10.1007/s00289-013-1029-6

Kamat, V., Bodas, D., & Paknikar, K. (2016). Chitosan nanoparticles synthesis caught in action using microdroplet reactions. *Scientific Reports*, *6*, 22260. http://doi.org/10.1038/srep22260

Kashyap, P. L., Xiang, X., & Heiden, P. (2015). Chitosan nanoparticle based delivery systems for sustainable agriculture. *International Journal of Biological Macromolecules*, *77*, 36–51. http://doi.org/10.1016/j.ijbiomac.2015.02.039

Krasnici, S., Werner, A., Eichhorn, M. E., Schmitt-Sody, M., Pahernik, S. A., Sauer, B., & Dellian, M. (2003). Effect of the surface charge of liposomes on their uptake by angiogenic tumor vessels. *International Journal of Cancer*, *105*(4), 561–567. http://doi.org/10.1002/ijc.11108

López-León, T., Carvalho, E. L. S., Seijo, B., Ortega-Vinuesa, J. L., & Bastos-González, D. (2005). Physicochemical characterization of chitosan nanoparticles: Electrokinetic and stability behavior. *Journal of Colloid and Interface Science*, *283*(2), 344–351. http://doi.org/10.1016/j.jcis.2004.08.186

Li, L., Chen, D., Zhang, Y., Deng, Z., Ren, X., Meng, X., & Zhang, L. (2007). Magnetic and fluorescent multifunctional chitosan nanoparticles as a smart drug delivery system. *Nanotechnology*, *18*(40), 405102. http://doi.org/10.1088/0957-4484/18/40/405102

Liu, G., Shao, L., Ge, F., & Chen, J. (2007). Preparation of ultrafine chitosan particles by reverse microemulsion. *China Particuology*, *5*(6), 384–390. http://doi.org/10.1016/j.cpart.2007.08.002

Lopez-Quintela, M. A. (2003). Synthesis of ordered mesoporous materials using surfactant liquid crystals or micellar solutions. *Current Opinion in Colloid and Interface Science*, *8*, 137–144. http://doi.org/10.1016/S1359-0294

Masarudin, M. J., Cutts, S. M., Evison, B. J., Phillips, D. R., & Pigram, P. J. (2015). Factors determining the stability, size distribution, and cellular accumulation of small, monodisperse chitosan nanoparticles as candidate vectors for anticancer drug delivery: Application to the passive encapsulation of [14C]-doxorubicin. *Nanotechnology, Science and Applications*, *8*, 67–80. http://doi.org/10.2147/NSA.S91785

Mi, F. L., Kuan, C. Y., Shyu, S. S., Lee, S. T., & Chang, S. F. (2000). Study of gelation kinetics and chain-relaxation properties of glutaraldehyde-cross-linked chitosan gel and their effects on microspheres preparation and drug release. *Carbohydrate Polymers*, *41*(4), 389–396. http://doi.org/10.1016/S0144-8617(99)00104-6

Mitra, S., Gaur, U., Ghosh, P. C., & Maitra, A. N. (2001). Tumour targeted delivery of encapsulated dextran-doxorubicin conjugate using chitosan nanoparticles as carrier. *Journal of Controlled Release*, *74*(1–3), 317–323. http://doi.org/10.1016/S0168-3659(01)00342-X

Monsan, P., Puzo, G., & Mazarguil, H. (1975). The study of the mechanism of establishment of glutaraldehyde-protein bonds. *Bioehimique*, *57*, 1281–1292.

Monsan, P. (1978). Optimization of glutaraldehyde support for enzyme immobilization. *Journal of Molecular Catalysis*, *3*, 371–384. http://doi.org/10.1002/jcp.23960

Monteiro, O. A. C., & Airoldi, C. (1999). Some studies of crosslinking chitosan-glutaraldehyde interaction in a homogeneous system. *International Journal of Biological Macromolecules*, *26*(2–3), 119–128. http://doi.org/10.1016/S0141-8130(99)00068-9

Nagpal, K., Singh, S. K., & Mishra, D. N. (2010). Chitosan nanoparticles: A promising system in novel drug delivery. *Chemical & Pharmaceutical Bulletin*, *58*(11), 1423–1430. http://doi.org/10.1248/cpb.58.1423

Nakata, M. (1997). Novel analysis of static light scattering data. *Polymer*, *38*(1), 9–13. http://doi.org/10.1016/S0032-3861(96)00471-5

Nie, S., Xing, Y., Kim, G. J., & Simons, J. W. (2007). Nanotechnology applications in cancer. *Annual Review of Biomedical Engineering*, *9*(1), 257–288. http://doi.org/5

Pa, J., & Yu, T. L. (2001). Light scattering study of chitosan in acetic acid aqueous solutions. *Macromolecular Chemistry and Physics*, *202*, 985–991. http://doi.org/10.1002/1521-3935(20010401)202:7<985:AID-MACP985>3.0.CO;2-2

Parent, M. E., Yang, J., Jeon, Y., Toney, M. F., Zhou, Z. L., & Henze, D. (2011). Influence of surfactant structure on reverse micelle size and charge for nonpolar electrophoretic inks? *Langmuir*, *27*(19), 11845–11851.

Pileni, M. P. (2007). Control of the size and shape of inorganic nanocrystals at various scales from nano to macrodomains. *Journal of Physical Chemistry C*, *111*(26), 9019–9038. http://doi.org/10.1021/jp070646e

Piletic, I. R., Tan, H., & Fayer, M. D. (2005). Dynamics of nanoscopic water: Vibrational echo and infrared pump-probe studies of reverse micelle. *Journal of Physical Chemistry B*, *109*(45), 21273–21284.

Poon, L., Wilson, L. D., & Headley, J. V. (2014). Chitosan-glutaraldehyde copolymers and their sorption properties. *Carbohydrate Polymers*, *109*, 92–101. http://doi.org/10.1016/j.carbpol.2014.02.086

Pujana, M. A., Pérez-Álvarez, L., Iturbe, L. C. C., & Katime, I. (2012). Water dispersible pH-responsive chitosan nanogels modified with biocompatible crosslinking-agents. *Polymer (United Kingdom)*, *53*(15), 3107–3116. http://doi.org/10.1016/j.polymer.2012.05.027

Qi, L., Xu, Z., Jiang, X., Hu, C., & Zou, X. (2004). Preparation and antibacterial activity of chitosan nanoparticles. *Carbohydrate Research*, *339*(16), 2693–2700. http://doi.org/10.1016/j.carres.2004.09.007

Qian, L., & Zhang, H. (2010). Green synthesis of chitosan-based nanofibers and their applications. *Green Chemistry*, *12*(7), 1207.
Rivas-Araiza, R., Alcouffe, P., Rochas, C., Montembault, A., & David, L. (2010). Micron range morphology of Physical chitosan hydrogels. *Langmuir*, *26*(22), 17495–17504. http://doi.org/10.1021/la102907u
Solanki, A., Kim, J. D., & Lee, K.-B. (2008). Nanotechnology for regenerative medicine: nanomaterials for stem cell imaging? *Nanomedicine*, *3*(4), 567–578.
Sorlier, P., Rochas, C., Morfin, I., Viton, C., & Domard, A. (2003). Light scattering studies of the solution properties of chitosans of varying degrees of acetylation. *Biomacromolecules*, *4*(4), 1034–1040. http://doi.org/10.1021/bm034054n
Stepankova, V., Bidmanova, S., Koudelakova, T., Prokop, Z., Chaloupkova, R., & Damborsky, J. (2013). Strategies for stabilization of enzymes in organic solvents. *ACS Catalysis*, *3*, 2823–2836.
Suh, J. K., & Matthew, H. W. (2000). Application of chitosan-based polysaccharide biomaterials in cartilage tissue engineering: a review. *Biomaterials*, *21*, 2589–2598. http://doi.org/10.1016/S0142-9612(00)00126-5
Swierczewska, M., Han, H. S., Kim, K., Park, J. H., & Lee, S. (2016). Polysaccharide-based nanoparticles for theranostic nanomedicine. *Advanced Drug Delivery Reviews*, *99*, 70–84. http://doi.org/10.1016/j.addr.2015.11.015
Tallury, P., Kar, S., Bamrungsap, S., Huang, Y.-F., Tan, W., & Santra, S. (2009). Ultra-small water-dispersible fluorescent chitosan nanoparticles: synthesis, characterization and specific targeting. *Chemical Communications (Cambridge, England)*, *17*, 2347–2349. http://doi.org/10.1039/b901729a
Tang, Z., Shangguan, D., Wang, K., Shi, H., Sefah, K., Mallikratchy, P., & Tan, W. (2007). Selection of aptamers for molecular recognition and characterization of cancer cells selection of aptamers for molecular recognition and characterization of cancer cells. *Analytical Chemistry*, *79*(13), 4900–4907.
Zhang, H., Oh, M., Allen, C., & Kumacheva, E. (2004). Monodisperse chitosan nanoparticles for mucosal drug delivery. *Biomacromolecules*, *5*(6), 2461–2468. http://doi.org/10.1021/bm0496211
Zhao, X., Hilliard, L. R., Mechery, S. J., Wang, Y., Bagwe, R. P., Jin, S., & Tan, W. (2004). A rapid bioassay for single bacterial cell quantitation using bioconjugated nanoparticles? *Proceedings of the National Academy of Sciences of the United States of America*, *101*(42), 15027–15032.
Zhi, J., Wang, Y., & Luo, G. (2005). Adsorption of diuretic furosemide onto chitosan nanoparticles prepared with a water-in-oil nanoemulsion system. *Reactive and Functional Polymers*, *65*(3), 249–257. http://doi.org/10.1016/j.reactfunctpolym.2005.06.009
Zhou, Z., Jiang, F., Lee, T. C., & Yue, T. (2013). Two-step preparation of nano-scaled magnetic chitosan particles using Triton X-100 reversed-phase water-in-oil microemulsion system. *Journal of Alloys and Compounds*, *581*, 843–848. http://doi.org/10.1016/j.jallcom.2013.07.207
Zou, P., Yang, X., Wang, J., Li, Y., Yu, H., Zhang, Y., & Liu, G. (2016). Advances in characterisation and biological activities of chitosan and chitosan oligosaccharides. *Food Chemistry*, *190*(12), 1174–1181.